

# 25<sup>TH</sup> INTERNATIONAL NORTH SEA FLOW MEASUREMENT WORKSHOP

October 16-19, 2007, Oslo, Norway

## Erosion in a Venturi Meter with Laminar and Turbulent Flow and Low Reynolds Number Discharge Coefficient Measurements

Gordon Stobie, ConocoPhillips

Robert Hart and Steve Svedeman, Southwest Research Institute<sup>®</sup>

Klaus Zanker, Letton-Hall Group

### 1.0 ABSTRACT

Venturi meters are commonly used in single and multiphase flows. The ISO standard (ISO 5167-4) provides meter discharge coefficients for Venturi meters in turbulent flows with Reynolds numbers above  $2 \times 10^5$ . In viscous fluids, Venturi are sometimes operated in laminar flows at Reynolds numbers below the range covered by the standards. Venturi meters may also be subjected to erosion from sand entrained in the fluid. The effects of erosion on the Venturi meter performance is a concern for long-term field operations.

Test data were obtained on a classical Venturi meter operating in laminar flow to measure the discharge coefficient as a function of Reynolds number. Data were obtained over a range of flow rates and fluid viscosities. Modeling using computational fluid dynamics (CFD) was used to obtain additional insight into the Venturi meter performance in laminar flow conditions. The test setup and test results are presented, with the CFD modeling results.

Tests were also conducted to evaluate the effects of erosion on Venturi meters. Three Venturi meters were exposed to oil/sand and water/sand slurry erosion. The meters were flow tested before and after exposure to the slurry flows to measure changes in the meter discharge coefficients. Dimensional changes were also recorded.

### 2.0 INTRODUCTION

This paper describes the measurement of Venturi meter discharge coefficients at low Reynolds numbers (with viscous oil) and presents the results for tests conducted to determine the effect of solid particle erosion in Venturi meter measurements.

**Discharge Coefficients.** Viscous oil production is sometimes metered using multiphase meters that contain Venturi flow elements. The conditions encountered in metering viscous fluids can be beyond the range of applicability of the industry standards (ISO 5167-4). The ISO standard is limited to turbulent flows for Reynolds numbers (based on the upstream pipe diameter) above  $2 \times 10^5$ . Metering viscous oils may involve laminar, rather than turbulent flow at Reynolds numbers below the range covered by the ISO standard.

A test program was carried out at the Southwest Research Institute (SwRI<sup>®</sup>) Multiphase Flow Facility to determine the discharge coefficient of a nominal four-inch diameter Venturi flow meter at low Reynolds numbers (approximately 80 to 100,000), in single-phase viscous flows. In addition, simulations were conducted using CFD to model the Venturi meter performance.

**Erosion.** Field experience has shown that heavy oil production is often associated with sand production, and erosion of the flow meters is not uncommon in these cases. It is not known

how meter erosion affects the venturi flow meter performance. In order to investigate the effect of erosion on Venturi meter accuracy, tests were conducted to erode Venturi meters.

Two test facilities were assembled at SwRI. The first was a water flow rig that was used to measure the discharge coefficients of the test meters before and after erosion. The second was to run viscous oil containing sand through the Venturi meters. The Venturi meters were exposed to the oil slurry erosion three times and the meter discharge coefficients were measured after each slurry exposure. After the slurry exposure, the meter dimensions were re-measured to determine any dimensional changes.

### 3.0 VENTURI METER DISCHARGE COEFFICIENTS

Per ISO 5167-4, the mass flow rate in a Venturi meter ( $q_m$ ) is given by:

$$q_m = \frac{C}{\sqrt{1-\beta^4}} \varepsilon \frac{\pi}{4} d^2 \sqrt{2(P_1 - P_2)\rho_1} \quad (1)$$

where:

C = Venturi discharge coefficient

$\beta$  = Venturi beta ratio,  $d/D$

d = Venturi throat diameter

D = Pipe diameter upstream of the Venturi convergent section

$\varepsilon$  = Expansion factor

$P_1$  = Static pressure at the upstream pressure tap

$P_2$  = Static pressure at the Venturi throat tap

$\rho_1$  = Fluid density at the upstream tap location

When working with Venturi meters, Reynolds numbers based on inlet pipe diameter (D) and throat diameter (d) are frequently used. These are defined as follows:

$$Re_D = \frac{\rho V D}{\mu} \quad (2A)$$

$$Re_d = \frac{\rho V d}{\mu} \quad (2B)$$

where  $\mu$ ,  $\delta$  and V are the dynamic viscosity, density, and average velocity, respectively, corresponding to either D or d.

Equation (1) is based on the assumptions that include steady, incompressible, and inviscid flow (no frictional pressure losses) and turbulent flow profiles (i.e., “flat” flow profiles) occur at the pressure tap locations. Two of the assumptions inherent in the Venturi equation do not apply when metering viscous fluids under laminar flow conditions. These are the assumptions that the flow is turbulent, so the velocity profile is uniform across the cross-section, and that the frictional pressure losses within the meter can be neglected.

Little data are available on Venturi discharge coefficients in laminar flow. Published results show that when the Reynolds number decreases below approximately  $2 \times 10^5$ , there is a small increase in the discharge coefficient before there is a steady decrease with decreasing Reynolds number. The strong dependence of the discharge coefficient on Reynolds number, for low Reynolds number flows makes it critical to know the operational conditions (so Reynolds number is known) for accurate metering.

A series of tests were conducted to obtain additional data on Venturi discharge coefficients under laminar flow conditions for Reynolds numbers below  $2 \times 10^5$ . The meter used was a four-inch ISO 5167-4 Venturi (Fluidic Techniques Model V-100) with a  $21^\circ$  convergent section and an  $8^\circ$  divergent section (included angles). Experiments were conducted over a range of flow rates and fluid viscosities. Dimensional details of the Venturi meter, were:  $D = 3.826$  inches,  $d = 2.399$  inches, and  $D = 0.627$  inches.

In addition, CFD modeling was conducted to to simulate laminar flow in a Venturi meter. The objectives was to gain additional insight into low Reynolds number flows in Venturi meters to evaluate how well CFD modeling can predict the experimental results.

### 3.1 Experimental Setup

Testing was conducted in the flow loop at the SwRI Multiphase Flow Facility. Although the flow loop can be configured to accommodate multiphase flows, the testing did not require gas flow, so the loop was operated in single-phase flow. A heat exchanger controlled the loop temperature. Figure 1 shows a photograph of the test facility.



Figure 1. SwRI Multiphase Flow Facility Flow Loop

The Venturi meter was installed in the flow loop downstream of a pair of reference flow meters. These were a Coriolis meter (Endress-Hauser Promass® 83F) to measure the density of the oil, and a positive displacement flow meter (Metroval FA 600-SR) that was the volumetric flow rate reference.

The Venturi meter instrumentation consisted of a static pressure transmitter and a pair of “stacked” differential pressure (DP) transmitters. Low-range (0-50 inH<sub>2</sub>O) and a high-range (0-250 inH<sub>2</sub>O) DP transmitters were installed to reduce the uncertainty at low flow rates. The flowing temperature at the meter was determined from an RTD located in the pipe immediately downstream of the Venturi flow meter.

Since oil viscosity is a function of temperature, it was necessary to establish the viscosity versus temperature relationship of the oil so that the Reynolds number could be accurately determined at the various operating temperatures. For this a laminar flow viscometer was used. The viscometer consisted of 5/8-inch OD tubing with two pressure taps (for measuring pressure drop) located a known distance apart. To control the temperature of the oil in the viscosity test section, the tubing was strapped to the main test section piping and insulated. Before and after each series of test runs, flow would be diverted through the viscometer to measure the viscosity at the operating conditions. An average temperature associated with each measured viscosity was determined from RTDs located at the upstream and downstream ends of the viscometer. Using the measured DP and the mass flow rate and density from a Coriolis flow meter installed in the viscometer, the viscosity ( $\mu$ ) was calculated using the following equation:

$$\mu = \left( \frac{\pi}{128} \right) \frac{\rho \Delta P D_v}{ML} \quad (3)$$

where:

- $\rho$  = Fluid density
- $\Delta P$  = Differential pressure between viscometer taps
- $D_v$  = Inside diameter of viscometer tube
- $M$  = Mass flow rate
- $L$  = Distance between viscometer taps

### 3.2 Test Conditions

For most of the testing, the flow loop was filled with Texaco Regal R&O 32 oil and pressurized with nitrogen. The static pressure in the loop was maintained between 150 and 200 psig over the course of the testing. (For each individual test run, the pressure was fixed.) Because of the difficulty in separating the gas from the viscous oil, care was taken to prevent the gas used to pressurize the loop from becoming mixed with the oil and carried to the test section. At the conclusion of the testing with oil, the loop was drained and filled with fresh water and a few test points were collected to check the performance of the Venturi meters in turbulent flow at higher Reynolds numbers. No effort was made to completely remove all oil from the loop, so the water was likely mixed with a small amount of oil.

132 test points were collected. Of these, 121 test points were completed with the oil and 11 were conducted with water. Table 1 summarizes the range of conditions covered.

**Table 1. Range of Conditions for the Venturi Meter Testing.**

METER SIZE	TEST FLUID	NUMBER OF TEST POINTS	Re <sub>d</sub>	TEMPERATURE [°F]	REFERENCE FLOWRATE [kg/s]
4"	Oil	121	80 - 8514	53 - 123	1.9 - 19.9
	Water	11	22,110 - 100,914	87 - 89	3.5 - 17.2

### 3.3 General Test Procedure

Testing consisted of a number of datasets, with each dataset corresponding to a different nominal temperature (and oil viscosity). Each dataset was in turn, composed of a number of individual test points taken at different flow rates (and Reynolds numbers). For each test point, the discharge coefficient was computed by dividing the reference mass flow rate by the Venturi meter mass flow rate as calculated from Equation (1) with  $C = 1$ . As the temperature of the oil

tended to change over the course of a dataset, each dataset was bracketed by viscosity measurements made at the beginning and end of the dataset. All of the viscosity measurements were combined to create a viscosity-versus-temperature relationship that was used in post processing to calculate Reynolds numbers for the measured temperature of each test point.

### 3.4 Experimental Results

The objective was to measure the discharge coefficient of the Venturi meter over a range of Reynolds numbers, primarily in the laminar flow regime. The calculation of the discharge coefficient was straightforward as it depended only on measured and geometric parameters, such as flow rate, differential pressure, and meter dimensions. The calculation of Reynolds number was complicated by the fact that in addition to geometric and measured quantities, it also depends on the oil viscosity. Since oil viscosity is a function of temperature and the oil temperature tended to vary between test points, the Reynolds number needed to be determined during a particular test run.

**Viscosity Measurements.** The approach used for calculating Reynolds numbers for the tests with oil was to combine all of the viscosity measurements to determine a functional relationship between viscosity and temperature and then use this relationship to calculate a Reynolds number for each test point based on the average measured temperature during that run.

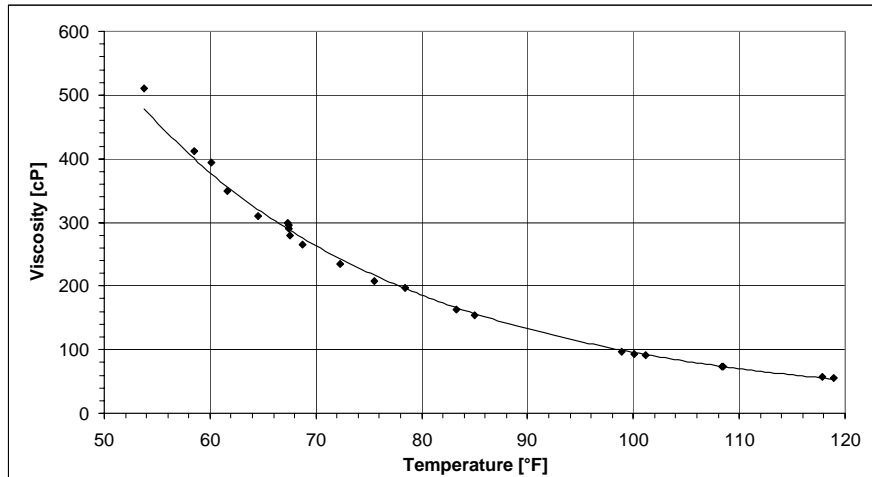


**Figure 2. Oil Viscosity as a Function of Temperature.**

Figure 2 presents the oil viscosity measurements with the curve fit that was used to characterize the data. The curve fit is of the form:

$$\mu = Ae^{B/T_{abs}} \quad (4)$$

which is the viscosity-versus-temperature model suggested by Fox and McDonald<sup>2</sup> for liquids. In Equation (4), A and B are constants and  $T_{abs}$  is the absolute temperature. A least-squares curve fit of all of the oil viscosity data points is shown as a solid line in Figure 2. Based on this fit, the values of the adjustable parameters in Equation (4) are as follows:

$$A = 1.72618 \times 10^{-6}$$

$$B = 9980.58$$

This curve fits the experimental data with an error that varies from -6.4% to +4.6%. The percentage error was calculated from the difference between each measured value of viscosity and the predicted value from the curve fit. Although this curve does not appear to fit the data

well at the highest viscosity (where there is a -6% error), the fit curve interpolates the remainder of the data points fairly well with errors that range from -4.8% to +4.6%.

**Discharge Coefficients.** The discharge coefficients for the Venturi meter are shown in Figure 3. The points below Reynolds number of 10,000 were obtained using oil as the test fluid, water was used for the points above 10,000. When plotted against the throat Reynolds number, the discharge coefficients, which were measured at a variety of temperatures, flow rates, and viscosities, all collapse onto a single curve. The overall behavior of the discharge coefficient curve is consistent with what is described in the literature and ISO 5167-4, including the “hump” that occurs as the Reynolds number decreases below 5,000. This hump is associated with the laminar-turbulent transition in the meter as explained by Benedict and Wyler<sup>3</sup>. At the highest Reynolds numbers, the experimental discharge coefficients agree with the values given in the ISO standard (0.970-0.977 for  $5 \times 10^4 < Re_d < 1 \times 10^5$ ). The uncertainty in the Reynolds number is estimated to be  $\pm 1.3\%$ , for all Reynolds numbers, and the uncertainty in the Venturi meter discharge coefficient ranges from approximately  $\pm 0.3\%$  to  $\pm 0.8\%$ .

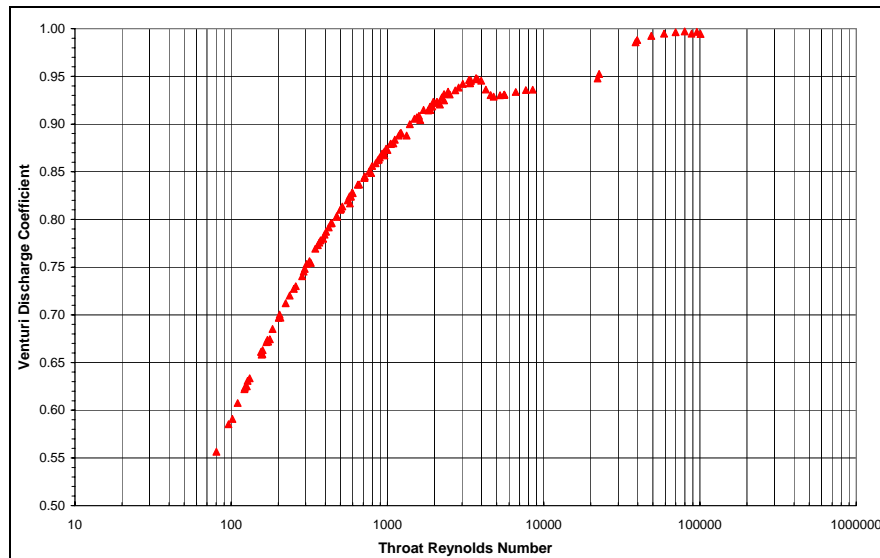


**Figure 3. Experimentally-Determined Discharge Coefficients for the Four-Inch Venturi Meter.**

In Figure 4, the discharge coefficients for the Venturi meter are compared to published data from several sources. Miller<sup>4</sup> presents data for  $40 \text{ mm} \leq D \leq 100 \text{ mm}$  and  $0.3 \leq \beta \leq 0.7$ , and the curve in Figure 4 is plotted assuming  $\beta = 0.5$ . Benedict and Wyler<sup>3</sup> proposed a generalized discharge coefficient for differential pressure-type flow meters. Figure 4 shows their proposed equation for laminar flow in a classical Venturi tube. The equations proposed by Pal<sup>5</sup> for the discharge coefficients for both stable and unstable water/oil emulsions are included, along with the data of Atkinson<sup>6</sup>.

The discharge coefficients follow the same general trends as the published results, but do not agree exactly with any of the correlations. For Reynolds numbers below about 1,000, the data falls within the range of the various published results. Between Reynolds numbers of 1,500 to 5,000, the experimental points tend to be higher than the correlations would predict, but above a Reynolds number of 5,000 there is, good agreement. The transition “hump” found in the data of Miller is also seen in the experimental data, although it does not occur at the same Reynolds number. Since laminar to turbulent transition is facility dependent and does not occur at a

specific Reynolds number, it is not surprising that there would be some differences in the published and experimental discharge coefficients in the transitional range of Reynolds numbers.

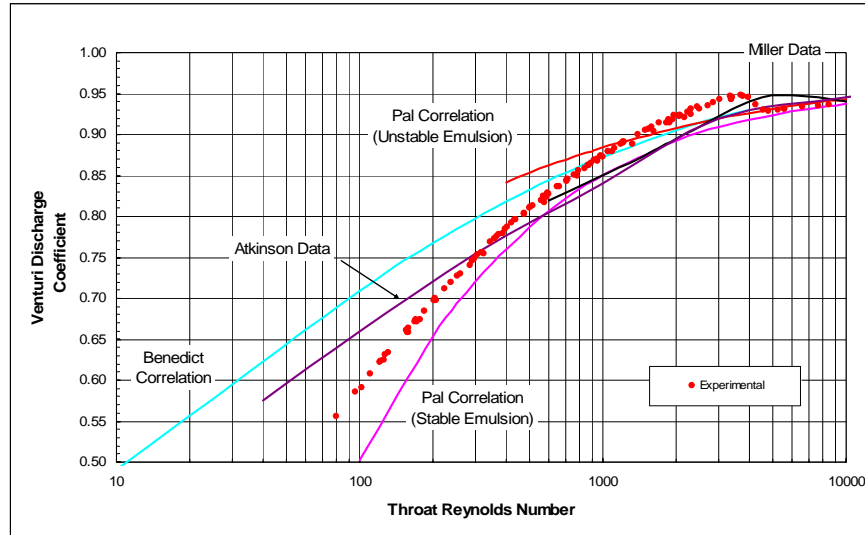


**Figure 4. Comparison of Published Values of Venturi Meter Discharge Coefficients for Low Reynolds Numbers with the Experimental Results.**

### 3.5 CFD Modeling

CFD modeling is a useful tool to gain an insight into the physics of the flow and to help understand the test results. The objective of the CFD work was to model the flow using two-dimensional CFD to obtain information about the flow that could not be obtained in the experimental test program. The CFD results were validated by running simulations for conditions within the range of the experimental test data and comparing the predicted discharge coefficients with the experimentally-determined values. Additional CFD simulations were conducted to predict Venturi meter operation at Reynolds numbers lower than could be simulated in the laboratory.

**Model Description.** The Fluent™ CFD model was used to simulate laminar flow through a Venturi meter. The Venturi geometry was modeled as a two-dimensional axisymmetric domain using a structured grid. The geometry was taken from the manufacturer’s drawing of the Venturi meter. No pressure taps were included in the CFD geometry.

Figure 5 shows the CFD grid used for the contraction section of the meter. The modeled geometry included five diameters of straight pipe upstream of the contraction section and a diffuser section. A total of 41 grid points were used to detail the radial direction, and a total of about 450 grid points were placed along the inlet pipe, contraction section, and diffuser.

In simulating a fully-developed laminar flow profile at the Venturi meter inlet, a laminar velocity profile was prescribed at the pipe inlet, located five D upstream of the upstream pressure tap. This ensured a fully-developed laminar velocity profile at the Venturi upstream pressure tap location. The flow solutions were obtained for steady, incompressible flow.

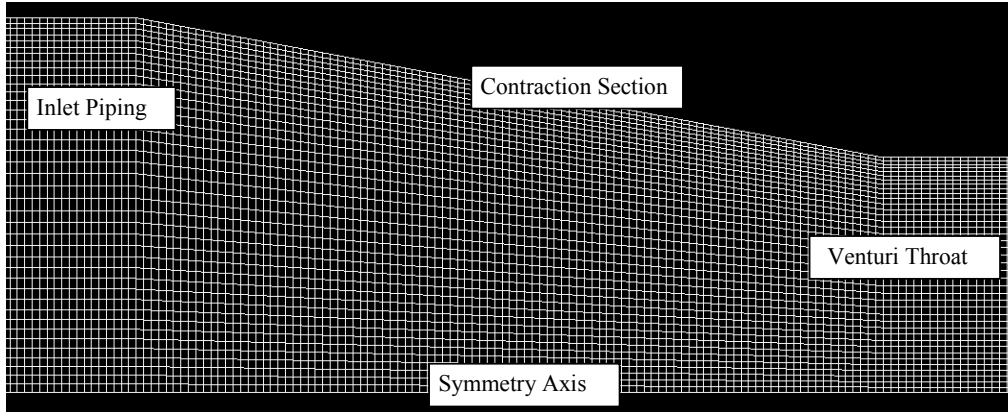


Figure 5. Computational Grid Used for the Contraction Section of the Venturi Meter Simulation.

**Discharge Coefficients.** CFD simulations were performed over a range of conditions. Venturi discharge coefficients were calculated from the predicted Venturi pressure drops and the flow rates. The simulations were done for oil viscosities of 250 cp, 500 cp, and 1,000 cp, a constant oil density of  $889.9 \text{ kg/m}^3$  (27.5 API), and Reynolds numbers from 34 to 1,654.

Figure 6 shows the test data and the CFD results plotted together. The agreement between the experimental and CFD results is good; although it appears that the curves represented by the two sets of data have slightly different slopes. The results appear to cross between Reynolds numbers of 100 to 200, with the CFD slightly underpredicting the discharge coefficient for Reynolds numbers above 200. The CFD simulations were done before the experiments, and the CFD data was not “tweaked” to achieve the level of agreement shown.

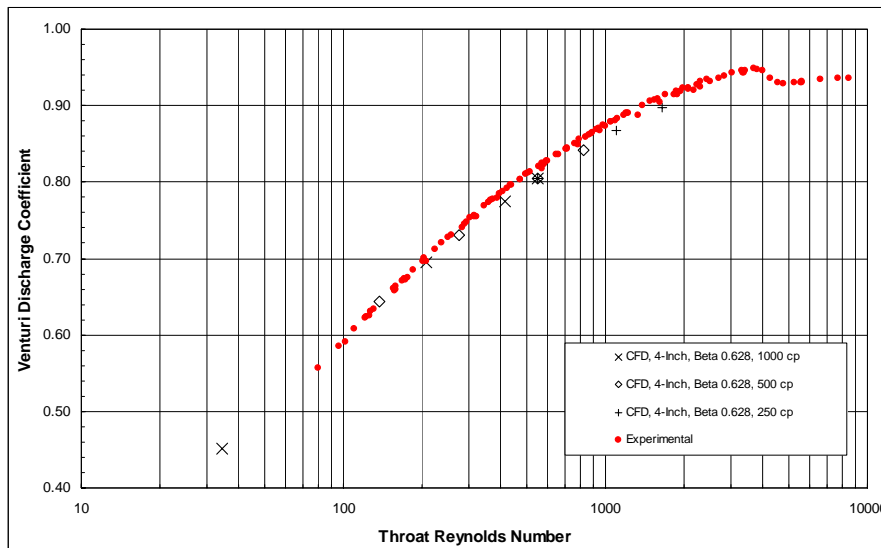
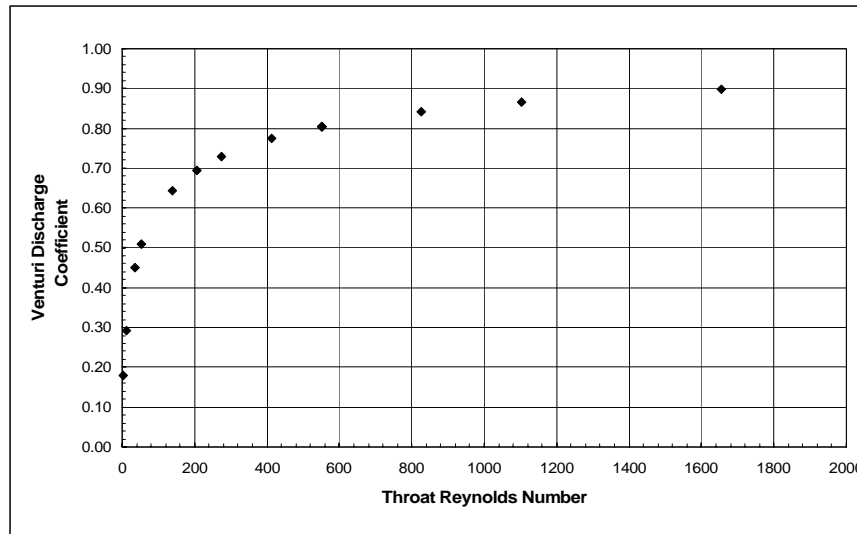


Figure 6. Comparison of Experimentally-Determined Venturi Meter Discharge Coefficients with the CFD Predictions.

Additional CFD simulations were carried out to predict Venturi discharge coefficients for Reynolds numbers below those that could be achieved experimentally. In these simulations, oil viscosities were increased to 30,000 cp to produce throat Reynolds numbers as low as two. The results show that the discharge coefficient tends toward zero as the Reynolds number is reduced. The discharge coefficient curve becomes very steep for Reynolds numbers below about 100.

These trends can be better seen when the data is plotted on a linear scale, as shown in Figure 7. One consequence of the nonlinear discharge coefficient curve is that a given uncertainty in the Reynolds number (viscosity or density uncertainty) will produce a larger uncertainty in the calculated discharge coefficient as the Reynolds number decreases.



**Figure 7. Venturi Meter Discharge Coefficient Versus Throat Reynolds Number Plotted Using a Linear Scale.**

**Frictional Pressure Loss.** A large portion of the pressure drop measured across the Venturi pressure taps is due to frictional forces at the low Reynolds numbers used in the simulations. Figure 8 shows the frictional pressure loss as a percentage of the total pressure drop. At Reynolds numbers below about 50, about one-half of the measured pressure drop in the Venturi is due to frictional losses. These results show that one of the key assumptions (inviscid flow) inherent in Equation (1) is obviously not valid for viscous oil under laminar flow conditions.

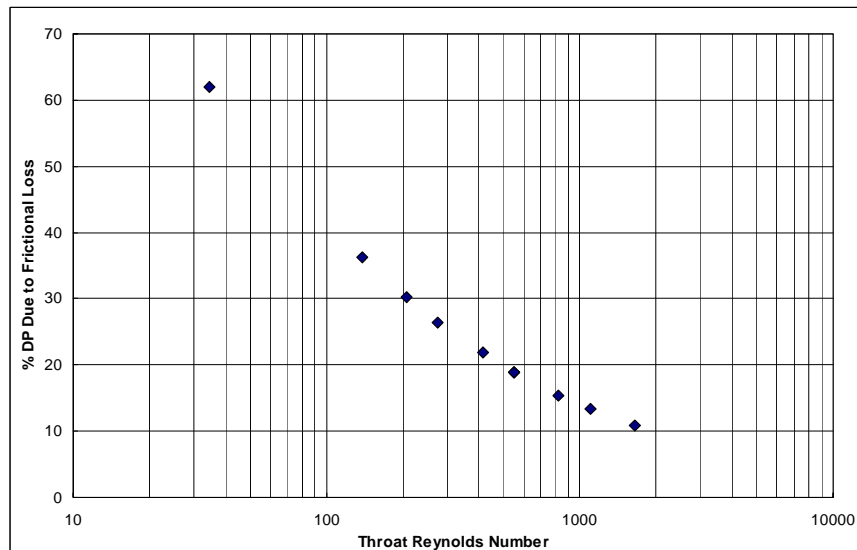


**Figure 8. Percentage of the Measured Venturi Pressure Drop Due to Frictional Pressure Loss.**

**Throat Velocity Profile.** CFD simulations were used to determine the kinetic energy correction factors at the Venturi throat pressure tap. Using the symbol  $v$  for the local velocity and  $V$  for the average velocity, the kinetic energy correction factor is defined as:

$$\alpha = \frac{1}{A} \int_A \left( \frac{v}{V} \right)^3 dA \quad (5)$$

The kinetic energy correction factor depends upon the velocity profile. For a fully-developed laminar flow profile,  $\alpha$  is equal to exactly two. For a fully-developed turbulent flow profile,  $\alpha$  will vary from about 1.02 for smooth pipe with a high Reynolds number to 1.2 for rough pipe at a lower Reynolds number. In most engineering computations for turbulent flow, the correction factor is usually neglected (set to equal 1.0), which is equivalent to assuming that the velocity profile is uniform.

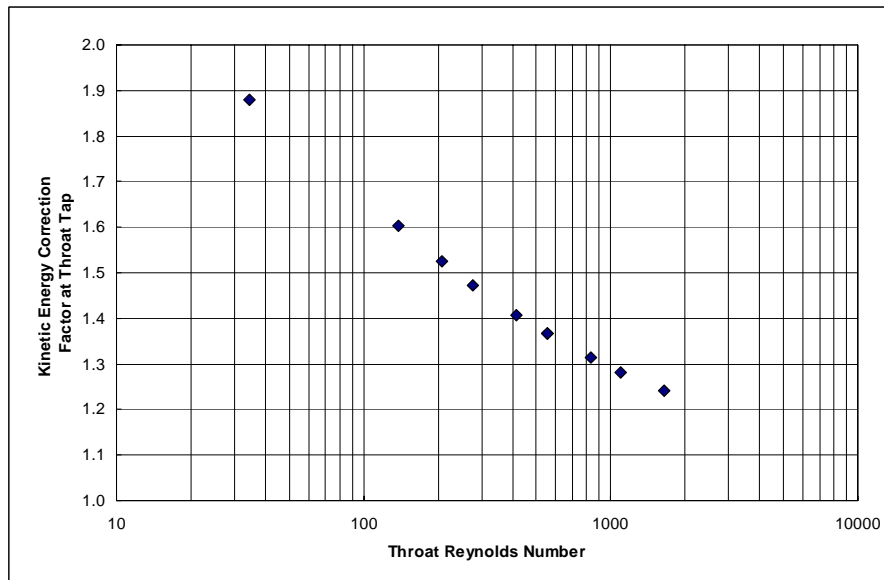


**Figure 9. Kinetic Energy Correction Factor for the Venturi Meter Throat Pressure Tap.**

Figure 9 shows the values of  $\alpha$  as a function of the throat Reynolds number. The kinetic energy correction factor  $\alpha$  varied from almost two at  $Re_d \sim 16$  to 1.2 at  $Re_d \sim 2,000$ . As expected, as the Reynolds number increased, the throat velocity profile became flatter, approaching a turbulent velocity profile with an  $\alpha$  value near 1. These results show that the second key assumption (flat or uniform velocity profile at the pressure taps) inherent in Equation (1) is not valid for viscous oil under laminar flow conditions.

#### 4.0 VENTURI EROSION TESTS

Erosion tests were conducted to determine how erosion of the Venturi effects flow meter performance. The objective of the work was to subject Venturi meters to a viscous fluid stream containing sand to determine where Venturi meters eroded. The effect of erosion on the measurement accuracy of Venturi meters was determined by flow testing the meters before and after exposure to the erosive flow stream. Dimensional measurements of the Venturi meters were recorded before and after exposure to the erosive flow stream. After the oil slurry erosion tests were completed, additional erosion testing was conducted using a water/sand slurry.

Four identical Venturi meters were used in the test program. One meter, the “standard” meter, was not exposed to the erosive flow conditions. The “standard” meter was used to compare the discharge coefficients of the other three meters before and after each erosion test. The flow tests were to identify any shifts in the eroded meters’ discharge coefficients. These flow tests were conducted using water flow and the Venturis were installed in accordance with ISO 5167-4 (straight pipe runs upstream and downstream of the Venturis).

Measurements were also made of the inside surfaces of the Venturi meters before and after the erosion tests to document changes to the surface finish and geometry.

**4.1 Pressure Tap Hole Imperfection in Venturi V-2586-1A.** In establishing the baseline discharge coefficients of the test meters, it was observed that one meter had a discharge coefficient of 0.973. This was significantly different from the other meters which were close to 0.995.

Visual inspection did not reveal any obvious defects. The problem was traced to a small burr on the upstream side of the “B” throat pressure tap. A casting of the pressure tap was made with a casting material so that the pressure tap contour could be seen (the throat tap was difficult to inspect since was located ~8” from the end flanges in a 1” diameter throat). Figure 10 shows a view of the casting at the intersection of the Venturi throat and the pressure tap. The burr stood up into the throat about 0.002”.

The burr was sanded down and the flow test repeated. The meter discharge coefficient changed from 0.973 to 0.999, a change of about +2.6%. The surface roughness measurement upstream of the pressure tap changed from 43 micro-inches before sanding to 11 micro-inches after sanding. It is possible that the smoother surface finish may have affected the discharge coefficient after sanding (the discharge coefficients of the test meters were determined relative to an identical Venturi that was assumed to have a discharge coefficient of 0.995).

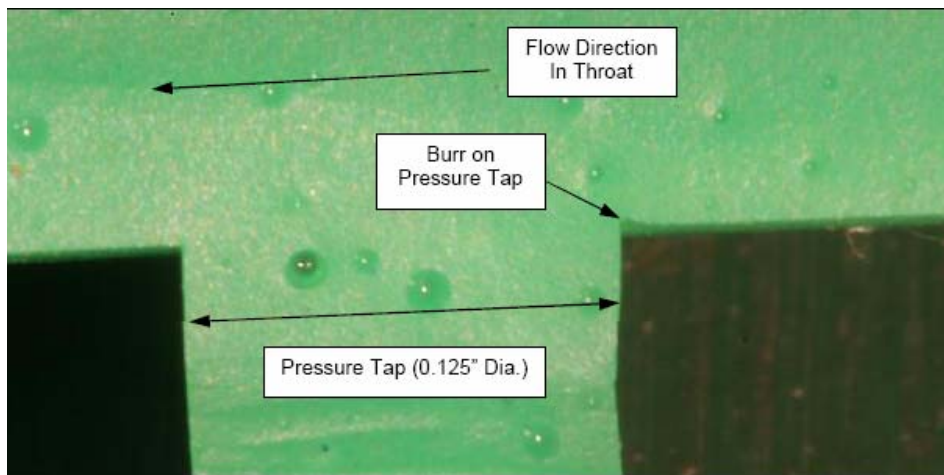


Figure 10: Burr on Venturi Meter V-2586-1A

#### 4.2 Erosion Test Rig and Test Meters

An erosion test rig was set up to flow viscous oil-sand slurry through the Venturi meters to simulate the erosion exposure of the meters under field conditions. Three Venturi meters were installed in series, so each of the meters was exposed to the same fluid flow and sand loading. A schematic of the test rig is shown in Figure 11.

The Venturi meters were installed vertically with the flow passing through the Venturis in the upward direction. The Venturis were installed directly downstream of blind tees as they would typically be installed in multiphase flow meters. The geometry for the flow meter installation is shown in Figure 12.

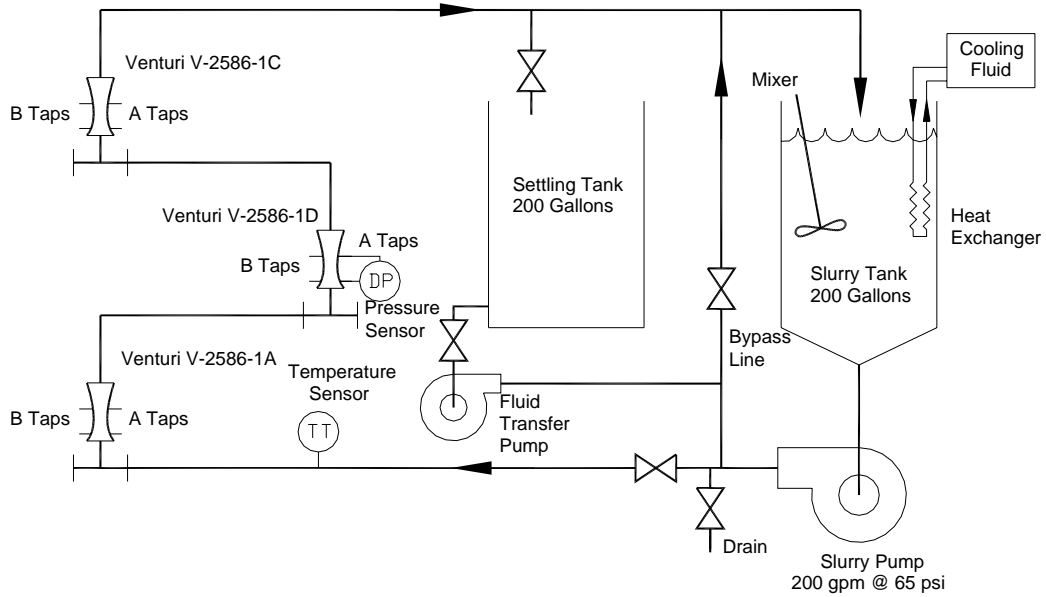


Figure 11. Schematic Diagram of the Erosion Test Rig.

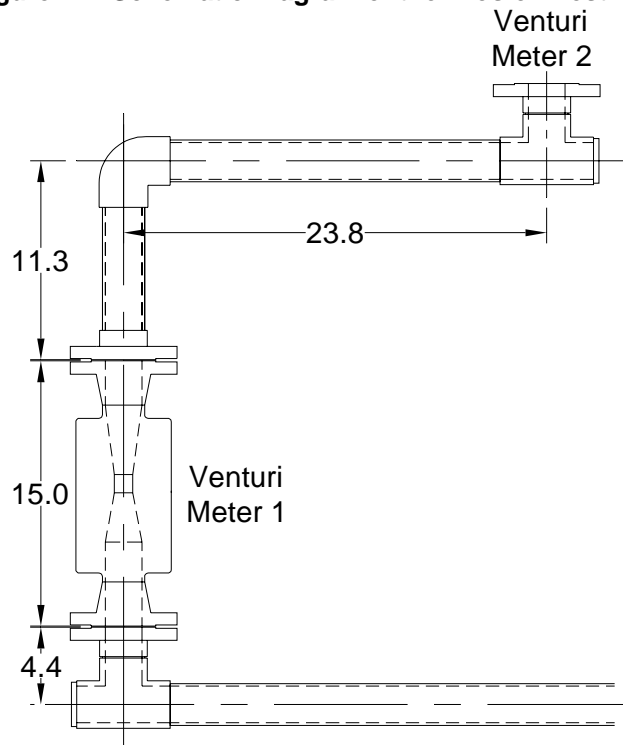


Figure 12. Flow Meter Installation Geometry.

**Test Meters.** Four matching Venturi meters were fabricated in 316 stainless steel, and is were designed to ISO 5167-4. The Venturis had a nominal two-inch inlet with 150# RF flanges and a Beta ratio of 0.5.

**Solid Particles.** The sand used for the erosion tests had a mean diameter of 276 microns. Figure 13 shows the result of a laser particle size analysis of the sand. The sand grains range in size from about 125 microns to about 600 microns. A photograph of the sand used in the tests is shown in Figure 14. The sand was made from crushed silica, so the particles were irregularly shaped and had sharp edges.

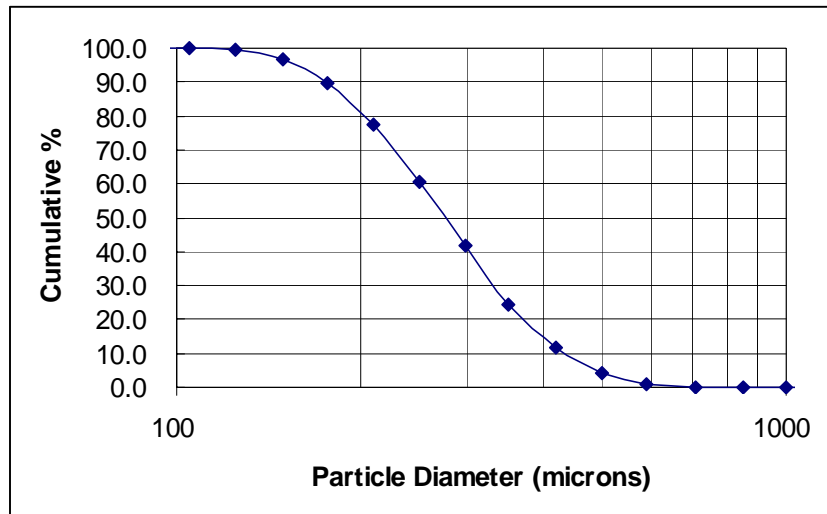


Figure 13. Plot of the Size Distribution of the Sand Used in the Erosion Tests.

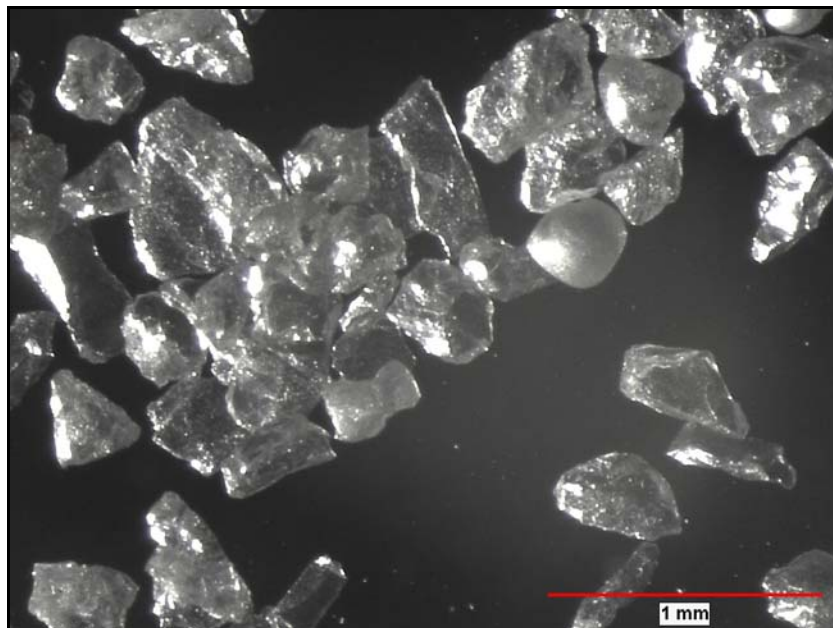


Figure 14. Photograph of the Sand Used in the Erosion Tests.

#### 4.3 Viscous Oil Erosion Tests

The erosion test conditions were selected to accelerate the erosion rate. To maximize erosion, a high sand loading was used along with a minimal fluid viscosity, and as high a flow

rate as possible. The test conditions required a tradeoff between laminar flow, increasing the flow rate, and minimizing viscosity.

The erosion tests were run at 120 gpm (about 4100BPD), oil viscosity of 360 cP, oil density of 0.88 gm/cm<sup>3</sup> and a sand loading of 2% to 4% by mass. For these conditions, the pipe Reynolds number was 450 and the throat Reynolds number was 900. The meter pressure drop during the test was ~16 psi (1.1 bar). The pipe velocity was about 11 ft/sec and the throat velocity was 46 ft/sec.

The Venturi meters were exposed to oil slurry erosion over three separate periods. Between each period, the Venturi meters were removed and installed in the water flow loop to determine any changes in the discharge coefficients. A summary of the conditions during each of the three erosion runs is given in Table 2.

**Table 2. Summary of the Erosion Test Conditions.**

CONDITION	EROSION RUN 1	EROSION RUN 2	EROSION RUN 3
Run Time (hr)	28.13	145.80	140.41
Average Sand Concentration (% by wt)	1.63	4.73	4.52
Average Temperature (°F)	107.8	107.3	107.5
Fluid Viscosity (cP)	357	364	362
Throat Reynolds No.	918	882	892
Venturi Throat Velocity (ft/sec)	45.8	45.2	45.8
Venturi Inlet Velocity (ft/sec)	11.4	11.3	11.5
Mass of Sand Through Venturis (lbm)	24,400	368,000	344,000

The total mass of sand that passed through each Venturi during Run 1 was 24,400 lbm. After Run 1, the Venturi discharge coefficients did not indicate any erosion, so the duration of the erosion test and the sand concentration in the slurry were increased. At the end of test Run 3, the three Venturi meters had had a total of 732,000 lbm of sand pass through them.

The oil flow tests after each erosion run showed no measurable change in the discharge coefficient. The dimensional measurements made before and after the erosion tests also showed no measurable erosion.

Photographs taken of the pressure taps before and after the erosion tests confirmed that the viscous slurry had not produced any significant erosion of the Venturi bores. Figure 15 shows photographs of the throat tap for one of the Venturis before the erosion test and after completing Run 3. The flow direction in the photograph is from the bottom to the top. The photographs show that the tap hole geometry was unchanged and the surface of the Venturi around the tap hole still has visible machine grooves after the erosion tests. Figure 16 shows a photograph of a throat pressure tap hole after exposure to the erosion tests. A 0.124-inch diameter rod was inserted into the tap hole to provide a dimensional reference. The 0.125-inch diameter pressure tap hole had not changed due to erosion. The machine grooves on the bore are also still visible, indicating that there was no significant erosion of the Venturi throat.

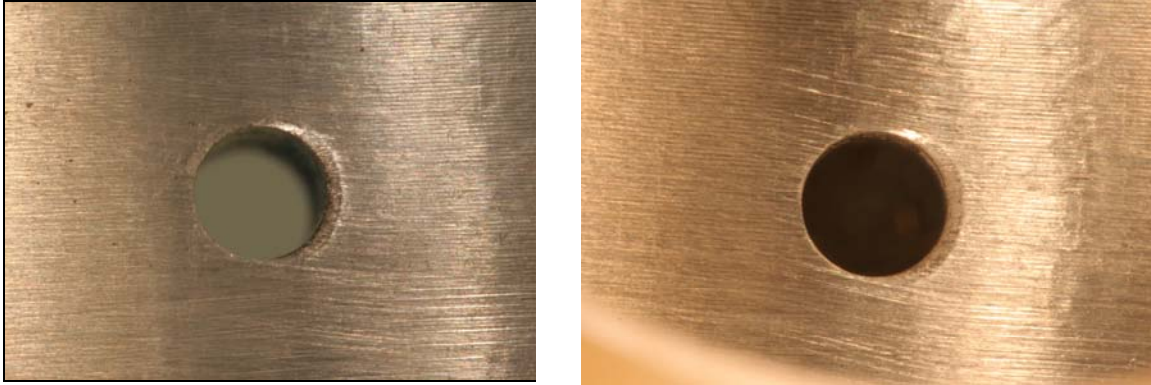


Figure 15. Upstream “A” Tap on Venturi V-2586-1D Before (L) and After (R) Exposure to the Sand Slurry.



Figure 16. Throat Tap (“A” Tap) in Venturi V-2586-1A after the Erosion Tests.

#### 4.4 Water Erosion Tests

After completing the oil slurry tests, further tests were conducted to expose the Venturi meters to a water/sand slurry. This was conducted using the same test rig, and sand size as the oil erosion tests. Total run time was 242 hours, and is summarized in Table 3.

Table 3. Flow Conditions for the Water/Sand Slurry Tests.

CONDITION	VALUE
Run Time (hr)	242
Average Sand Concentration (% by wt)	4.57
Average Temperature (°F)	77.5
Fluid Viscosity (cP)	0.884
Throat Reynolds No.	419,900
Venturi Throat Velocity (ft/sec)	44.7
Venturi Inlet Velocity (ft/sec)	11.2
Mass of Sand Through Venturis (lbm)	664,000

The total mass of sand that passed through each Venturi during the test was 664,000 lbm. The pipe water velocity during the test was 11.2 ft/sec and 44.7 ft/sec in the Venturi throat.

**Discharge Coefficient Shift.** The Venturi meter’s discharge coefficients were measured before and after the water/sand slurry test to document changes in the meters due to erosion.

Discharge coefficients were measured in the water flow rig. The three Venturi meters that were exposed to erosion were tested against the “standard” meter that was not exposed to the erosive flow. The discharge coefficient for the “standard” meter was assumed to be 0.995 and the other meters’ discharge coefficients were determined relative to the “standard” meter. Each Venturi had two sets of pressure taps located 180° apart. The two sets were labeled A and B Taps.

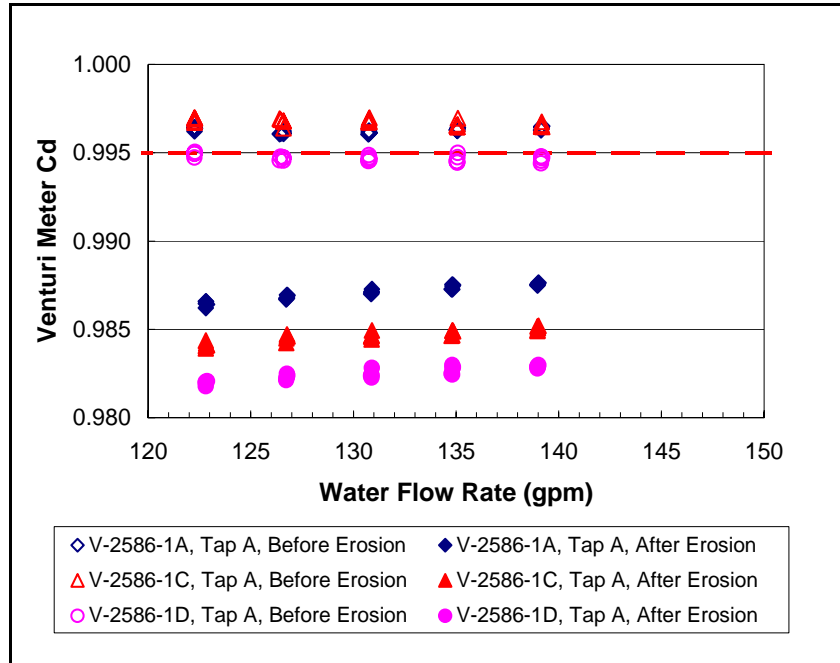


Figure 17. Venturi Meter Discharge Coefficients Measured Before and After the Water/Sand Slurry Exposure – “A” Taps.

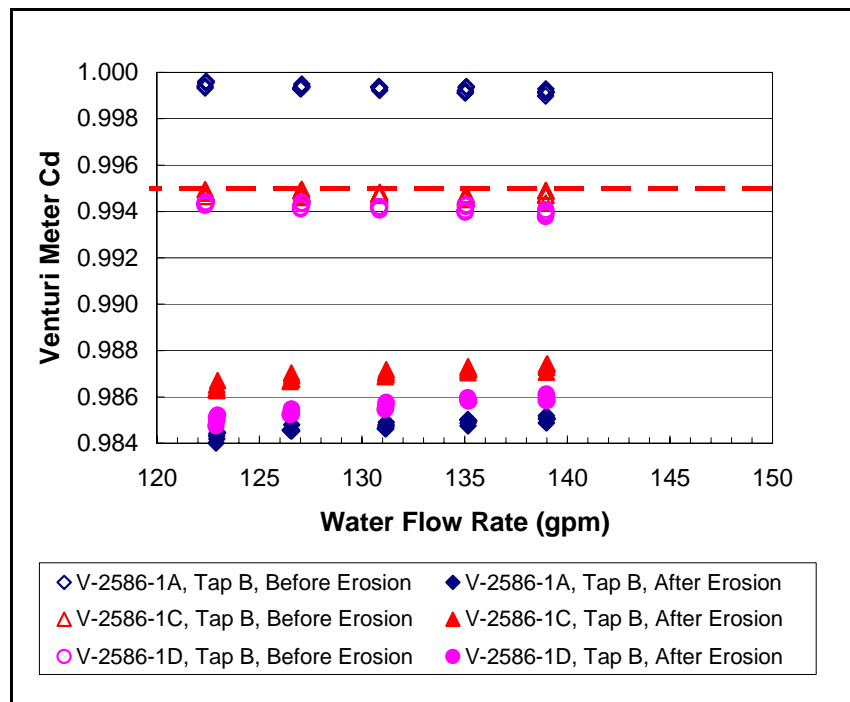


Figure 18. Venturi Meter Discharge Coefficients Measured Before and After the Water/Sand Slurry Exposure – “B” Taps.

The discharge coefficients measured before and after the water erosion test are shown in Figures 17 and 18. The discharge coefficients were measured in turbulent flow for a range of flow rates and at Reynolds numbers based on the pipe diameter between  $4 \times 10^5$  and  $5 \times 10^5$ . Figure 17 shows the meter discharge coefficients when the differential pressure was recorded using the “A” Taps and Figure 18 shows the discharge coefficients recorded using the “B” Taps. The meter erosion caused an average change in the discharge coefficient of about -1%. The discharge coefficients recorded after the erosion test were computed using the meter geometry measurements taken before the erosion test.

**Venturi Geometry Change.** Measurements were made of the Venturi meter pipe and throat diameters, and the surface roughness prior to exposing the meters to the water slurry flow and were repeated after the erosion test. The upstream diameter was measured near the upstream taps (3.52 inches from the upstream flange face) with an internal micrometer. Measurements were made with the micrometer oriented at  $0^\circ$ ,  $90^\circ$ ,  $180^\circ$ , and  $270^\circ$  relative to the “A” Taps. Measurements of the throat diameter were also recorded. The diameter was measured just upstream of the throat pressure tap at a location 7.86 inches from the upstream flange face. The throat bore had a slight taper (diameter reducing in the direction of flow), so additional diameter measurements were made at a location 8.30 inches from the inlet flange face. Table 4 lists the average dimensions for the three test Venturis.

**Table 4. Change in the Venturi Dimensions after the Water Erosion Test.**

VENTURI #	VENTURI DIAMETER AND CHANGE IN DIAMETER	DIAMETER AT UPSTREAM TAPS-AT 3.52" (INCH)	DIAMETER AT THROAT TAPS-AT 7.86" (INCH)	DIAMETER IN THROAT-AT 8.3" (INCH)
V-2586-1A	Average Diameter	2.0642	1.0333	1.0327
	Change in Diameter	-0.0010	-0.0048	-0.0151
V-2586-1D	Average Diameter	2.0659	1.0332	1.0323
	Change in Diameter	-0.0009	-0.0048	-0.0153
V-2586-1C	Average Diameter	2.0640	1.0333	1.0327
	Change in Diameter	-0.0008	-0.0041	-0.0140

The average diameter change at the upstream tap was an increase of about 0.001 inches (negative values in Table 4 indicate the bore diameter increased in testing). The diameter of the Venturi throat increased about 0.005” just upstream of the throat pressure tap.

Before the water erosion test, the Venturi throat had a slight taper with the diameter decreasing in the direction of flow. After the erosion test, the throat diameter increased in the direction of the flow. Figure 19 show a plot of the throat diameter measured at different locations along the throat (the throat inlet is 7.55 inches for the inlet flange face and the end of the throat is 8.57 inches from the inlet flange face). Based on extrapolating the measurements made before the erosion test, the throat diameter at the inlet increased approximately 0.001 inches. The diameter at the outlet end of the throat increased by about 0.020 inches.

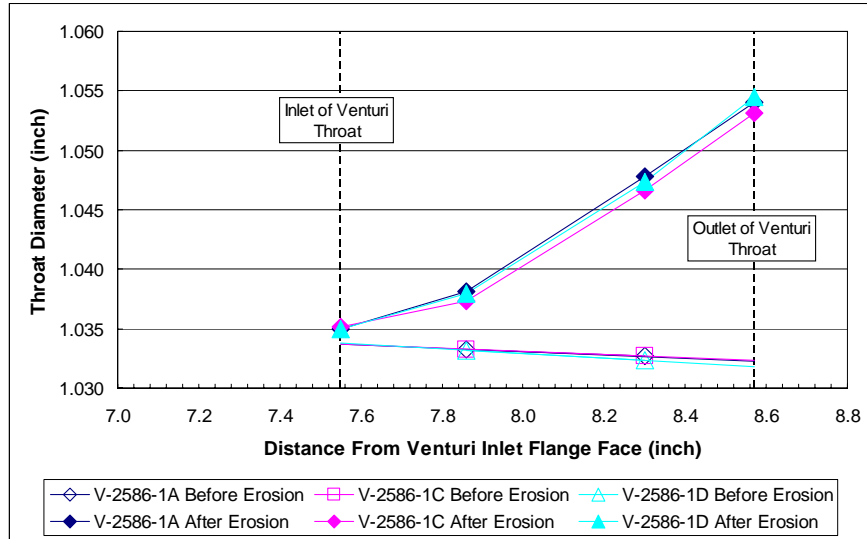


**Figure 19. Plot of the Venturi Throat Diameter Measurements Before (Open Symbols) and After (Solid Symbols) the Water Erosion Test.**

**Photographs of Erosion.**

**Upstream (pipe) Taps.** Photographs were taken of the pipe pressure taps after the water erosion test. There was considerable erosion on the downstream side of the tap holes. Figure 20 shows photographs of the upstream “A” and “B” pressure taps on Venturi V-2586-1C.

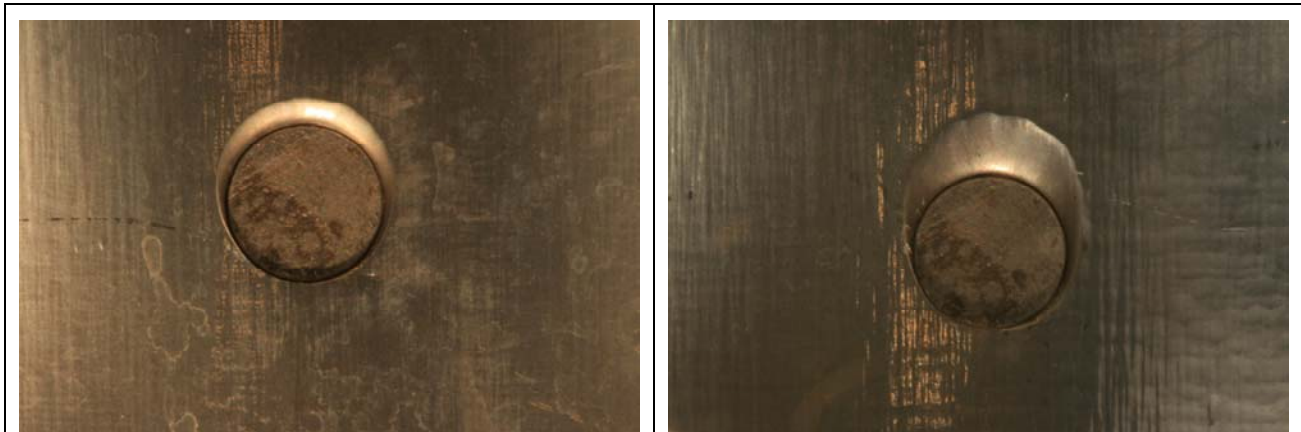


**Figure 20. Upstream “A” (L) and “B” (R) Taps on Venturi V-2586-1C After the Water Erosion Test.**

The direction of flow on the photographs is toward the top of the page. The “B” Tap had more erosion (right photograph, Figure 20) and was located on the outside of the flow bend created by the blind tee located just upstream of the Venturi. The upstream tap located on the outside of the flow bend had more erosion than the pressure tap located on the inside of the flow bend. This was true for all three Venturi meters.

The surface around the upstream pressure tap holes was eroded. The machine grooves that were visible before the erosion test (see Figure 15 for comparison) were eroded and erosion channels were cut into the surface, as seen in Figure 20. The eroded channels were aligned with the direction of the flow, which was towards the top of the photograph in Figure 20.

**Throat Taps.** The throat pressure taps were eroded by the water slurry. Figure 21 shows the downstream side (toward the top of the page) of the pressure tap, which was eroded into a shallow U-shaped cut. The surface around the throat taps was eroded smooth. The machine grooves visible before the erosion test were eroded away

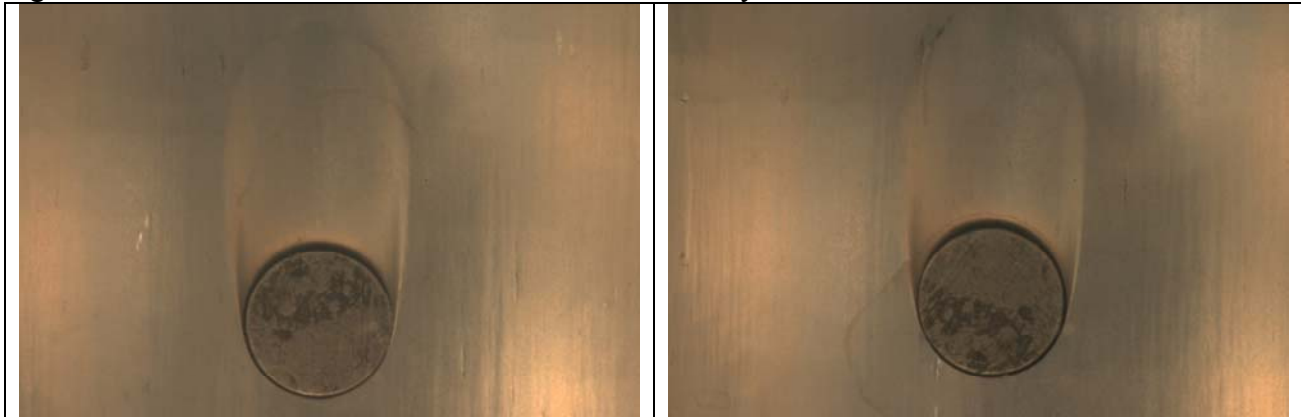


**Figure 21. Throat “A” (L) and “B” (R) Taps on Venturi V-2586-1C After the Water Erosion Test.**

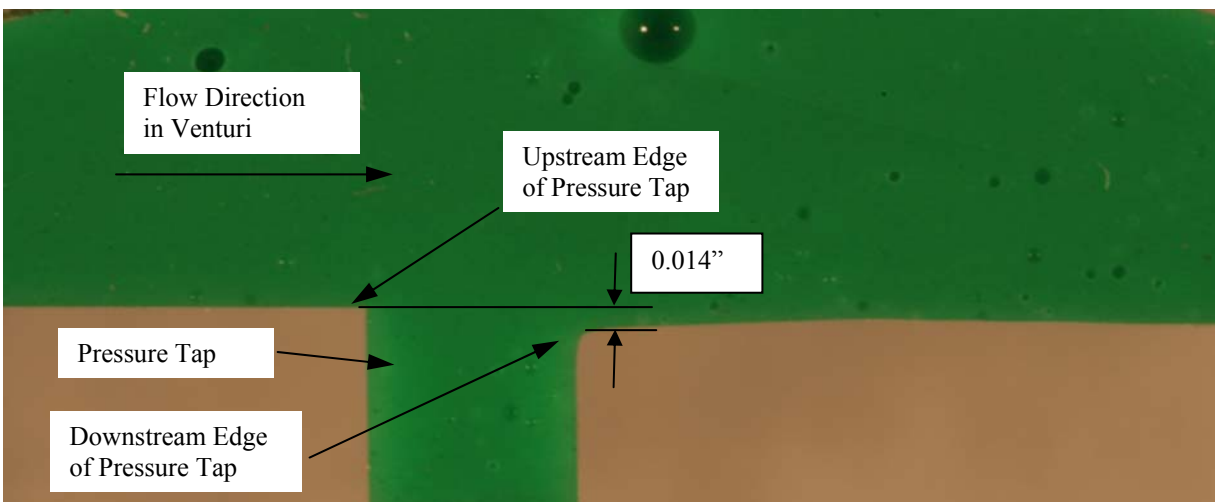


**Figure 22. Cross-Section Cut from a Casting of the “A” Throat Tap of Venturi V-2586-1A.**

A casting of the pressure tap and the throat surface around the pressure tap was made to determine the depth of erosion at the throat tap. Figure 22 shows a cross-section cut through the casting material. The cut plane passes through the centerline of the pressure tap and the plane was aligned with the direction of flow. The upstream edge of the pressure tap was sharp, but the downstream edge was eroded down by 0.014 inch below the upstream edge. The downstream edge had a radius of about 0.008 inch.

**Changes in Discharge Coefficient Change.** The discharge coefficients of the eroded meters changed by about -1% due to erosion. An increase in the throat diameter due to erosion would be expected to result in an increased discharge coefficient. The decrease in discharge coefficient was caused by the eroded pressure tap holes. The modified tap hole geometry increased the measured differential pressure to overcome the larger throat diameter and resulted in a decrease in the overall discharge coefficient.

If the erosion had only caused a change to the throat and upstream diameters, the shift in the discharge coefficient would have been expected to be about +1.8%. The shift in discharge coefficient that would result if only the pressure tap holes had eroded (no diameter change) was estimated to be about -2.5%.

Thus the diameter increase offset the changes caused by the pressure tap hole erosion.

## 5.0 CONCLUSIONS

Experiments were conducted on a four-inch Venturi flow meter over a range of flow rates and fluid viscosities with the objective of obtaining data on Venturi discharge coefficients under laminar flow conditions for a Reynolds number range below that given in ISO5167-4. Discharge coefficients were determined based on comparison of the calculated Venturi flow rate to the reference flow meter. In testing, both the flow rate and the temperature (and thus viscosity) were varied to obtain a range of Reynolds numbers that covered the laminar flow regime down to a Reynolds number of 80. The main conclusions reached from the investigation are:

- The discharge coefficients for the Venturi meter, fall on a single curve when correlated with the throat Reynolds number. This curve has a slight “hump” in the transitional range of Reynolds numbers before steadily decreasing as the Reynolds number is reduced. This is in contrast to the application of Venturi meters in turbulent flow, where the value of the discharge coefficient is taken as a constant.
- The discharge coefficients were compared to published correlations and it was found that the data followed the same general trends, but did not agree exactly with any of the correlations. The experimental discharge coefficients fell between the extremes defined by the various published results, except in the range of Reynolds numbers where transition from laminar to turbulent flow was occurring.

CFD modeling was performed to determine if CFD simulations could predict the performance of a Venturi flow meter under conditions typical of those encountered in metering viscous fluids. The CFD results were used to obtain detailed information on Venturi meter flow characteristics that could not be easily measured during experimental testing. Conclusions from the CFD modeling include:

- The agreement between the experimental and CFD results is good; although it appears that the two data sets have slightly different slopes. Comparisons with a range of experimental data were not made, the favorable agreement between the experimental and computational results suggests that CFD can be used to model the low Reynolds number flows when using Venturi meters.
- For laminar flow in a specific Venturi geometry (fixed  $D$  and  $\beta$ ), discharge coefficient is a function of the throat Reynolds number over a range of viscosities and flow rates.

Three 2 inch Beta ratio 0.5 venturi meters were erosion tested. The venturi meters were flow tested with water to determine their discharge coefficients. One meter exhibited an unusual discharge coefficient which was the result of a small burr on the throat tap. Removal of the burr restored the discharge coefficient. Venturi pressure taps are critical components, and small discontinuities can and will create anomalous data.

The erosion test results showed that erosion of Venturi meters by a viscous fluid-sand slurry was not a major concern. The smooth flow of fluid through the Venturi meter combined with the viscosity of the fluid limited the sand impact, reducing erosion of the Venturi meters.

Significant Venturi meter erosion was experienced when exposed to a water/sand slurry. The erosion test conditions were similar to the viscous oil tests with a flow rate of about 120gpm (4100BPD). The flow for the water erosion test was turbulent with a Reynolds number >400,000. The test ran for ten days and 664,000 lbm of sand passed through each meter. In production operations, this would indicate that as water cuts increase (or bulk viscosity is reduced) significant erosion may be possible when sand is produced.

Erosion caused about a 1% decrease in the Venturi meter's overall discharge coefficient.

- The pressure tap holes experienced significant erosion with the downstream side of the tap holes being badly eroded. It is thought that this could have impacted the meter discharge coefficient by -2.5%.
- The surface finish inside the Venturi meters changed from the machine finish to a smooth, eroded surface, and the throat bore was eroded. It is thought that this could have impacted the meter discharge coefficient by +1.8%.
- The throat tap is a sensitive part of the venturi meter with respect to performance change due to defects and and erosion.

Dimensional measurements after the erosion test showed the Venturi throat had a significant taper, with the outlet end having a diameter that was about 0.020inches larger than the inlet end. The throat inlet end, just downstream from the contraction section did not experience much erosion. It appears that the nature of the flow entering the throat moved the sand away from the contraction cone and limited the erosion at the throat inlet.

## 6.0 REFERENCES

1. ISO 5167-4, "Measurement of Fluid Flow by Means of Pressure Differential Devices Inserted in Circular Cross-Section Conduits Running Full – Part 4: Venturi Tubes," 2003.
2. Fox, R. W., and McDonald, A. T., *Introduction to Fluid Mechanics*, Wiley and Sons, New York, 1992.
3. Benedict, R. P., and J. S. Wyler, "A Generalized Discharge Coefficient for Differential Pressure Type Fluid Meters," ASME Journal of Engineering for Power, pp. 440-448, October 1974.
4. Miller, R. W., *Flow Measurement Engineering Handbook*, McGraw-Hill, New York, 1996.
5. Pal, R., "Flow of Oil-in-Water Emulsions through Orifice and Venturi Meters," *Industrial Engineering & Chemistry Research*, Vol. 32, pp. 1212-1217, 1993.
6. Atkinson, D. I., et al., "Qualification of a Nonintrusive Multiphase Flow Meter in Viscous Flow," SPE 63118, 2000 SPE Annual Technical Conference and Exhibition, Dallas, TX, October 1-4, 2000.